

Received 10 June 2024, accepted 23 June 2024, date of publication 2 July 2024, date of current version 12 July 2024.

Digital Object Identifier 10.1109/ACCESS.2024.3422097

RESEARCH ARTICLE

Adaptive Dynamic Surface Control for Uncertain Nonlinear Time-Delay Cyber-Physical Systems Under Injection and Deception Attacks

DANIAL ROSTAMI^{ID} AND MARZIEH KAMALI^{ID}

Department of Electrical and Computer Engineering, Isfahan University of Technology, Isfahan 84156-83111, Iran

Corresponding author: Marzieh Kamali (m.kamali@iut.ac.ir)

ABSTRACT Nowadays, cyber-physical systems (CPSs) have gained remarkable attention in electrical and control engineering. However, their vulnerability to attacks poses challenges for control. This report explores the adaptive dynamic surface control approach for CPSs against both injection and deception attacks on states and the control signal with unknown direction, suggesting using Nussbaum functions. Given the comprehensive nature of nonlinear time-delay CPSs, this research focuses on designing an adaptive resilient controller for such systems. To address the challenges of time-delay CPSs without restrictive assumptions, specific even functions are applied to resolve signal zeroing in the controller's denominator due to time-varying delays. Utilizing these functions in dynamic surface control, presents challenges that are addressed in this study. The proposed method ensures the boundedness of all closed-loop signals and two simulation examples are given to show how well it works.

INDEX TERMS Cyber-physical systems, injection and deception attacks, adaptive dynamic surface control, time-delay systems.

I. INTRODUCTION

Cyber-physical systems (CPSs) consist of two main components: physical elements such as sensors and actuators, and communication networks that are responsible for facilitating interactions between these physical elements, ensuring that communication aligns with controller-specified commands. CPSs are commonly found in various industries, including smart power grids, power plants, petrochemical industries, refineries, etc. Researchers worldwide are now focusing on projects involving CPSs because of their vital role and importance in human life.

These systems face numerous security threats which are caused by their network and cyber communications, making them susceptible to cyber-attacks. These attacks have the potential to disrupt the physical system. Thus, ensuring the security of communication networks and the robustness of the control system in CPSs is vital. Given the significance

The associate editor coordinating the review of this manuscript and approving it for publication was Zheng Chen^{ID}.

of CPSs, research on issues like attacks and defensive measures is crucial. Despite progress in system modeling, attack modeling, energy control, security, and controller design approaches, the study of CPSs and defense strategies against potential attacks is still in its early stages and research on their performance continues. CPSs face various attack types categorized into three groups: Denial of Service (DoS) attacks, injection and deception attacks, and replay attacks. Each is important in its own right and today, they have garnered special attention from the research community.

As previously mentioned, the investigation of CPSs remains a contentious and remarkable subject for researchers, given both their importance and susceptibility to attacks. In [1], [2], [3], [4], [5], and [6], a comprehensive examination of CPSs, including security gaps and available solutions to address and decrease these vulnerabilities, as well as strategies to counteract attacks, has been undertaken. In [7], [8], and [9], investigations and research have delved into control solutions for CPSs under DoS attacks, wherein attackers hinder the transmission of control signals or sensor-measured

signals by sending interfering signals or causing prolonged delays, resulting in system damage. Notably, [10], [11] have addressed replay attacks and explored suitable control approaches to defend against these attacks.

A prevalent category of attacks, central to this research, is injection and deception attacks. Injection attacks target sensor output signals, while deception attacks focus on control input signals, altering correct data during transmission and potentially causing system faults or even breakdowns. Therefore, one effective solution to compensate for changes caused by attacks in these systems is the use of the adaptive control approach. In [12], [13], and [14], adaptive control has been investigated for linear CPSs under deception attacks, injection attacks, and both injection and deception attacks, respectively. Given that some systems are inherently nonlinear and susceptible to malicious attacks, studying nonlinear CPSs under such threats has become a crucial area of investigation. In [15], an adaptive backstepping approach is used for nonlinear CPSs with unknown functions under injection attacks. Actually, [16], [17] investigated using the adaptive backstepping method for nonlinear CPSs with known nonlinear functions and uncertain parameters, under injection and deception attacks. Moreover, [18] explores using the adaptive dynamic surface control method in nonlinear CPSs under random injection attacks which can stabilize the system.

Given the inherent delays in some industrial systems, recent research has focused on developing defense strategies against attacks targeting these CPSs. In [19], a study explored adaptive dynamic surface control for nonlinear CPSs with time-varying state delays and unknown functions, considering injection and deception attacks in which the direction of attacks is known. Similarly, [20] examined an adaptive controller for nonlinear CPSs with time-varying delays in its states against injection attacks and actuator failures which controller ensures system stability.

The objective of this study is to design an adaptive and resilient controller for uncertain nonlinear CPSs with time-varying delays in states, influenced by injection and deception attacks with unknown direction. The main contributions of the article are summarized as follows:

1. In this research, we consider both injection attacks on states and deception attacks on the control signal for nonlinear time-delay CPSs with unknown functions. Given the delay and uncertainties of the nonlinear CPSs, addressing both these attacks complicates controller design. This article presents solutions to these challenges. To handle the issue of unknown signs of the multiplied signals in the states and control signal, special Nussbaum functions [21] are utilized.
2. The dynamics of the system investigated in this research are in the form of strict feedback but slightly more comprehensive. To the best of our knowledge, previous studies on this subject, such as [15], [16], [17], [18], [19], [20], [22], [23], and [24], have not

considered virtual coefficients and input coefficient for their systems. In this research, we consider bounded time-varying virtual coefficients in the states. This reduces the restriction on the dynamics of CPSs. Furthermore, uncertain disturbances are considered in the dynamics of the CPSs, so their bounds should be estimated. Our focus is also to design a robust controller for the system.

3. Considering uncertain time-varying delays in states poses challenges in control design, especially with signals in the controller's denominator. This can be addressed by introducing assumptions limiting system dynamics or applying relevant lemmas that could make the system sensitive. In this investigation, we utilize specific even functions in controller design for the first time in time-delay CPSs, resolving signal zeroing without additional assumptions.
4. The presence of the even functions mentioned in the previous item, in the design process, categorized stability proof into several cases. In the dynamic surface method, dealing with one more variable than the backstepping method, we face challenges in proving stability which we aim to resolve. Our approach involves using two positive semi-definite functions instead of a general positive definite function, ensuring the stability of the closed-loop system. Additionally, due to the step-by-step nature of this method, some uncertain parameters are related to subsequent steps and they can not be estimated easily in subsequent steps due to the existence of the even functions. We address this challenge by adding and subtracting these terms in the subsequent steps, allowing for the estimation of their uncertain parameters.

II. PROBLEM FORMULATION AND PRELIMINARIES

The dynamic model of CPSs represented in this essay is in the form of strict feedback with time-varying virtual coefficients given as

$$\begin{cases} \dot{\tilde{x}}_i = g_i(t)\tilde{x}_{i+1} + f_i(\tilde{x}_i) + h_i(\tilde{x}_{\bar{\tau}_i}) + d_i(t), i = 1, \dots, n-1 \\ \dot{\tilde{x}}_n = g_n(t)\tilde{u} + f_n(\tilde{x}_n) + h_n(\tilde{x}_{\bar{\tau}_n}) + d_n(t) \end{cases} \quad (1)$$

where $\tilde{x}_i = [\tilde{x}_{i1}, \dots, \tilde{x}_{in}]^T$ for $i = 1, \dots, n$, and $\tilde{x}_n \in \mathbb{R}^n$ and \tilde{u} are the system states and input signal, respectively. The vector $\tilde{x}_{\bar{\tau}_i} = [\tilde{x}_{i1}(t - \tau_1(t)), \dots, \tilde{x}_{in}(t - \tau_i(t))]^T$ represents the delayed states of the system. Here, $\bar{\tau}_i = [\tau_1(t), \dots, \tau_i(t)]^T$ denotes the unknown time-varying delay vector corresponding to system states. The virtual coefficients $g_i(t)$ are also unknown, time-varying, and bounded, with the condition $g_i(t) \neq 0$ for $i = 1, \dots, n$, and $\forall t \in \mathbb{R}^+$. Additionally, $d_i(t)$ represents the uncertain time-varying disturbance, $f_i(\tilde{x}_i)$, $i = 1, \dots, n$ are unknown continuous functions of system states, and $h_i(\tilde{x}_{\bar{\tau}_i})$, $i = 1, \dots, n$ represent unknown continuous functions of the delayed states of the system.

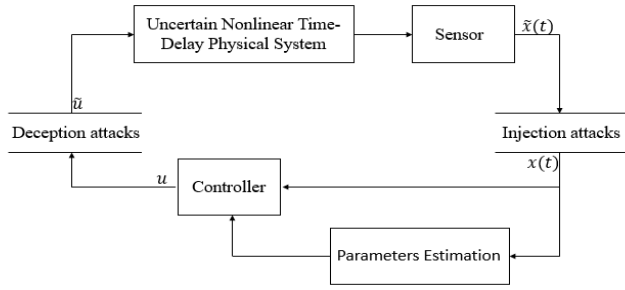


FIGURE 1. Schematic of closed-loop system, under cyber-attacks.

In this paper, we consider attacks conducted by attackers, to be injection and deception. These attacks impact both the signals transmitted from the sensors and the control signal directed to the actuator. The effects of attacks pose significant challenges to the control of the system which inherently has high uncertainty and time-varying virtual coefficients. So, the injection and deception attack on states and control input signal are modeled as

$$\begin{cases} x_i &= \tilde{x}_i + (w_i(t)) \tilde{x}_i \\ \tilde{u} &= b(t)u + v(t) \end{cases} \quad (2)$$

where $w_i(t) \in \mathbb{R}$ represents an unknown and time-varying injected signal designed by attackers with an unknown sign, $v(t) \in \mathbb{R}$ is an unknown attack parameter, $b(t) \in \mathbb{R}$ is an unknown attack multiplicative signal with an unknown sign and u is the control signal designed by the controller. According to the attacks, the true state signals \tilde{x}_i are not accessible to the control designer. Consequently, the controller signal must be designed by using false state signals x_i . The schematic of the closed-loop system and the procedure for controlling the nonlinear time-delay CPSs under injection and deception attacks are shown in Fig. 1.

If we assume $1 + w_i(t) = \lambda_i(t)$, the attacks on the system states can be expressed as $x_i = \lambda_i(t)\tilde{x}_i$ and $x_i(t - \tau_i(t)) = \lambda_i(t - \tau_i(t))\tilde{x}_i(t - \tau_i(t))$. Therefore, the dynamic equations describing the system during and after an attack are

$$\begin{cases} \dot{x}_i &= \dot{\lambda}_i(t)\lambda_i^{-1}(t)x_i + \lambda_i(t)g_i(t)\lambda_{i+1}^{-1}(t)x_{i+1} \\ &+ \lambda_i(t)f_i(\lambda_i^{-1}(t)x_i) + \lambda_i(t)h_i(\lambda_i^{-1}(t - \tau_i)x_{\tilde{\tau}_i}) \\ &+ \lambda_i(t)d_i(t), \quad i = 1, \dots, n-1 \\ \dot{x}_n &= \dot{\lambda}_n(t)\lambda_n^{-1}(t)x_n + \lambda_n(t)g_n(t)b(t)u + \lambda_n(t)g_n(t)v(t) \\ &+ \lambda_n(t)f_n(\lambda_n^{-1}(t)x_n) + \lambda_n(t)h_n(\lambda_n^{-1}(t - \tau_n)x_{\tilde{\tau}_n}) \\ &+ \lambda_n(t)d_n(t) \end{cases} \quad (3)$$

where $\lambda_i^{-1}(t)x_i$ is a vector defined as $[\lambda_1^{-1}(t)x_1, \dots, \lambda_i^{-1}(t)x_i]^T$, and $\lambda_i^{-1}(t - \tau_i)x_{\tilde{\tau}_i}$ is another vector can be defined as

$$\begin{aligned} &[\lambda_1^{-1}(t - \tau_1)x_1(t - \tau_1), \dots, \lambda_i^{-1}(t - \tau_i)x_i(t - \tau_i)]^T. \text{ Now let} \\ &\begin{cases} \mu_i(t) = \lambda_i(t)g_i(t)\lambda_{i+1}^{-1}(t), \quad i = 1, \dots, n-1 \\ \mu_n(t) = \lambda_n(t)g_n(t)b(t), \quad \mu_{n+1}(t) = \lambda_n(t)g_n(t)v(t) \end{cases} \end{aligned} \quad (4)$$

Therefore, the dynamic equations (3) could be rewritten as

$$\begin{cases} \dot{x}_i &= \dot{\lambda}_i(t)\lambda_i^{-1}(t)x_i + \mu_i(t)x_{i+1} + \lambda_i(t)f_i(\lambda_i^{-1}(t)x_i) \\ &+ \lambda_i(t)h_i(\lambda_i^{-1}(t - \tau_i)x_{\tilde{\tau}_i}) + \lambda_i(t)d_i(t) \\ \dot{x}_n &= \dot{\lambda}_n(t)\lambda_n^{-1}(t)x_n + \mu_n(t)u + \mu_{n+1} + \lambda_n(t)f_n(\lambda_n^{-1}(t)x_n) \\ &+ \lambda_n(t)h_n(\lambda_n^{-1}(t - \tau_n)x_{\tilde{\tau}_n}) + \lambda_n(t)d_n(t). \end{cases} \quad (5)$$

Assumption 1: The attacks are assumed to satisfy $b(t) \neq 0$ and $\lambda_i(t) \neq 0$ for all $i = 1, \dots, n$ at all times, implying $w_i(t) \neq -1$ for $i = 1, \dots, n$. Additionally, the signals $\lambda_i(t)$, $\lambda_i(t)$, $b(t)$, and $v(t)$ are bounded, but their bounds are unknown.

Remark 1: In many practical applications, attackers have restricted ability to manipulate the measurements of sensors and actuators due to the constraints of physical instruments. Consequently, assuming that the signals sent by attackers are bounded is reasonable [16]. On the other hand, although the assumption that $b(t) \neq 0$ and $\lambda_i(t) \neq 0$, $i = 1, \dots, n$, is a limitation, it is required to be able to implement the control signal to the system and make this approach feasible. Furthermore, it is a common assumption in this field [15], [16], [17], [18], [19], [20].

Assumption 2: The disturbance signals $d_i(t)$, $i = 1, \dots, n$, are time-varying and bounded with unknown boundaries and the indeterminate delay of states $\tau_i(t)$, $i = 1, 2, \dots, n$ is a differentiable function given by

$$0 \leq \tau_i(t) \leq \tilde{\tau}_i, \quad \dot{\tau}_i(t) \leq \kappa_i \leq 1, \quad \text{for } 1 \leq i \leq n. \quad (6)$$

Here, κ_i and $\tilde{\tau}_i$ are unknown parameters.

Remark 2: To address uncertain time-varying delays, we can impose assumptions on state functions involving delays [25], [26] or on the delays themselves [27], [28]. Since some CPSs may not meet the conditions for the functions, this essay focuses on restrictions on delays. By adopting this assumption, the Lipschitz condition is not required for the nonlinear functions of system dynamics.

Lemma 1 ([16]): Let $\gamma(x, y) \in \mathbb{R}$ be a continuous function, then there exist two continuous functions $\alpha(x) > 0$ and $\beta(y) > 0$ such that:

$$|\gamma(x, y)| \leq \alpha(x)\beta(y). \quad (7)$$

Lemma 2 ([19]): For the unknown function $h_i(\tilde{x}_{\tilde{\tau}_i})$ where $\tilde{x}_{\tilde{\tau}_i} = [x_1(t - \tau_1(t)), \dots, x_i(t - \tau_i(t))]^T$, there exist unknown continuous functions $\Xi_{i,l} \geq 0$ such that

$$|h_i(\tilde{x}_{\tilde{\tau}_i})| \leq \sum_{l=1}^i \Xi_{i,l}(x_l(t - \tau_l(t))). \quad (8)$$

Definition 1: A continuous function \mathcal{N} is called Nussbaum if the relations

$$\begin{cases} \limsup_{s \rightarrow \infty} \frac{1}{s} \int_0^s \mathcal{N}(\chi) d\chi = +\infty \\ \liminf_{s \rightarrow \infty} \frac{1}{s} \int_0^s \mathcal{N}(\chi) d\chi = -\infty \end{cases} \quad (9)$$

hold for it [21].

Definition 2 ([15]): The function $N(s) : \mathbb{R} \rightarrow \mathbb{R}$ is a specific form of the continuous Nussbaum function, denoted as $N(s) \in \mathcal{N}$. It satisfies certain conditions, expressed as

$$\begin{cases} \liminf_{k \rightarrow \infty} \frac{k - \int_0^k N^-(s) ds}{\int_0^k N^+(s) ds} = 0 \\ \liminf_{k \rightarrow \infty} \frac{k + \int_0^k N^+(s) ds}{-\int_0^k N^-(s) ds} = 0 \end{cases} \quad (10)$$

Here, $N^-(s)$ and $N^+(s)$ represent the negative and positive components of the function $N(s)$ respectively, defined as $N^+(s) = \max\{0, N(s)\}$ and $N^-(s) = \min\{0, N(s)\}$.

Nussbaum’s gain method has been utilized in various studies to address uncertainties in virtual coefficients and input coefficient. Ordinary Nussbaum functions may not effectively compensate for the unknown multiple time-varying virtual coefficients and input coefficient, as detailed in [15] and [21]. Therefore, to handle unknown time-varying coefficients $\mu_i(t)$ for $i = 1, \dots, n$, the special Nussbaum functions introduced in Definition 2 are used.

Lemma 3 ([29]): Consider the smooth and continuous functions $V(t)$ and $\chi_i(t)$, $i = 1, \dots, n$, in the interval $[0, t_f]$, where $\forall t \in [0, t_f]$, $V(t) \geq 0$, and $N(\chi_i)$ is the Nussbaum function. If the condition

$$\begin{aligned} V(t) \leq c_0 + e^{-c_1 t} \sum_{i=1}^n \int_0^t A_i(t) N(\chi_i) \dot{\chi}_i e^{c_1 \tau} d\tau \\ + e^{-c_1 t} \sum_{i=1}^n \int_0^t \dot{\chi}_i e^{c_1 \tau} d\tau \end{aligned} \quad (11)$$

is established, where $A_i(t)$ is an unknown, bounded, and nonzero parameter, c_1 is a positive constant, and c_0 is a constant value, it can be concluded that the signals $V(t)$, $\chi_i(t)$, and $\int_0^t g_i(t) N(\chi_i) \dot{\chi}_i d\tau$ are all bounded.

Lemma 4 ([27]): Let the even function, $q_i(s_i) : \mathbb{R} \rightarrow \mathbb{R}$ be defined as

$$q_i(s_i) = \begin{cases} 1, & |s_i| \geq \delta_{a_i} + \delta_{b_i} \\ C_{q_i} \int_{\delta_{a_i}}^{s_i} [(\delta_{a_i} + \delta_{b_i} - \sigma)(\sigma - \delta_{a_i})]^{(n-i)} d\sigma, & \delta_{a_i} < s_i < \delta_{a_i} + \delta_{b_i} \\ C_{q_i} \int_{s_i}^{-\delta_{a_i}} [-(\delta_{a_i} + \delta_{b_i} + \sigma)(\sigma + \delta_{a_i})]^{(n-i)} d\sigma, & -(\delta_{a_i} + \delta_{b_i}) < s_i < -\delta_{a_i} \\ 0, & |s_i| \leq \delta_{a_i} \end{cases} \quad (12)$$

where $\delta_{a_i}, \delta_{b_i} > 0$ are constant parameters that should be designed and $C_{q_i} = \frac{(2(n-i)+1)!}{\delta_{b_i}^{2(n-i)+1} [(n-i)!]^2}$, thus $q_i(s_i)$ is $(n-i)$ th differentiable and is limited between 0 and 1.

III. CONTROLLER DESIGN

In this section, the main focus is on designing a proper controller for the nonlinear time-delay CPSs under injection and deception attacks. The Adaptive Dynamic Surface Control method will be utilized to derive the final control law, which involves some steps. To design the controller, we perform a variable change as follows

$$\begin{cases} s_1 = x_1 \\ s_i = x_i - z_i, X_i = z_i - \alpha_{i-1}, \quad 2 \leq i \leq n \end{cases} \quad (13)$$

Here, s_i represents the error surface, z_i is the state variable obtained by passing the virtual controller α_{i-1} through a filter and X_i is the error of the mentioned filter output. This filter is represented as

$$\zeta_i \dot{z}_i + z_i = \alpha_{i-1}, \quad z_i(0) = \alpha_{i-1}(0) \quad (14)$$

where, ζ_i is the time constant of the filter. By using this and (13), the equation $\dot{z}_i = \frac{-X_i}{\zeta_i}$ can be easily obtained.

step 1: First, by considering (13), the dynamics of the first error surface according to the system (5) is

$$\begin{aligned} \dot{s}_1 = \dot{\lambda}_1(t) \lambda_1^{-1}(t) x_1 + \mu_1(t) x_2 + \lambda_1(t) f_1 \left(\overline{\lambda_1^{-1}(t) x_1} \right) \\ + \lambda_1(t) h_1 \left(\overline{\lambda_1^{-1}(t - \tau_1) x_{\bar{\tau}_1}} \right) + \lambda_1(t) d_1(t). \end{aligned} \quad (15)$$

Now, the non-negative function of the first subsystem is supposed to be $V_{s_1} = \frac{1}{2} s_1^2$. Its derivative with respect to time is $\dot{V}_{s_1} = s_1 \dot{s}_1$ which can be written as

$$\begin{aligned} \dot{V}_{s_1} = s_1 \left(\dot{\lambda}_1(t) \lambda_1^{-1}(t) x_1 + \mu_1(t) x_2 + \lambda_1(t) f_1 \left(\overline{\lambda_1^{-1}(t) x_1} \right) \right. \\ \left. + \lambda_1(t) h_1 \left(\overline{\lambda_1^{-1}(t - \tau_1) x_{\bar{\tau}_1}} \right) + \lambda_1(t) d_1(t) \right). \end{aligned} \quad (16)$$

By considering (13), let’s substitute $x_2 = s_2 + X_2 + \alpha_1$ and, by using the inequality $ab \leq \varepsilon a^2 b^2 + \frac{1}{4\varepsilon}$, where ε is a positive fixed value, (16) can be rewritten as

$$\begin{aligned} \dot{V}_{s_1} \leq \varepsilon_1 s_1^2 x_1^2 \left(\dot{\lambda}_1(t) \lambda_1^{-1}(t) \right)^2 + \mu_1(t) s_1 (s_2 + X_2 + \alpha_1) \\ + \varepsilon_1 s_1^2 \lambda_1^2(t) f_1^2 \left(\overline{\lambda_1^{-1}(t) x_1} \right) + \varepsilon_1 s_1^2 \lambda_1^2(t) d_1^2(t) \\ + s_1 \lambda_1(t) h_1 \left(\overline{\lambda_1^{-1}(t - \tau_1) x_{\bar{\tau}_1}} \right) + \frac{3}{4\varepsilon_1}. \end{aligned} \quad (17)$$

Now, considering assumption 1 and equation (4), the signals $\mu_i(t)$, $\mu_n(t)$, and $\mu_{n+1}(t)$ are bounded. To simplify the design of the controller, we introduce certain variables as

$$\begin{cases} \vartheta_i = \sup \left(\dot{\lambda}_i(t) \lambda_i^{-1}(t) \right)^2, \quad 1 \leq i \leq n-1 \\ \vartheta_n = \sup \left(\dot{\lambda}_n(t) \lambda_n^{-1}(t) \right)^2 \end{cases} \quad (18)$$

In addition, by applying Lemma 1, we are able to establish $\lambda_i^2(t) f_i^2 \left(\overline{\lambda_i^{-1}(t) x_i} \right) \leq \lambda_i^2(t) \bar{\omega}_i^2 \left(\lambda_i^{-1}(t) \right) \psi_i^2(\bar{x}_i)$. Since $\bar{\omega}_i^2$

is a non-negative continuous function and $\overline{\lambda_i^{-1}(t)}$ is a vector with bounded elements, there exists a constant ρ_i such that $\lambda_i^2(t)\overline{\omega_i^2}(\lambda_i^{-1}(t)) \leq \rho_i$. Furthermore, we define $\varphi_i(\bar{x}_i) = \psi_i^2(\bar{x}_i)$. To approximate the unknown functions $\varphi_i(\bar{x}_i)$, $i = 1, \dots, n$, we utilize Radial Basis Function (RBF) artificial neural networks, expressed as

$$\varphi_i(\bar{x}_i) = \varrho_i^T \phi_i(\bar{x}_i) + \epsilon_i \quad (19)$$

where $\phi_i(\bar{x}_i)$ represents vectors of Gaussian functions, ϱ_i denotes network weights and unknown coefficients vectors, and ϵ_i stands for the approximation error. Previous research [30] indicates that with a sufficient and suitable selection of the number of Gaussian functions in ϕ_i , the error is bounded as $\|\epsilon_i(x)\| \leq \epsilon_{M_i}$. Utilizing this expression and the inequality $ab \leq \frac{a^2}{2} + \frac{b^2}{2}$ and by using (18), equation (17) can be reformulated as

$$\begin{aligned} \dot{V}_{s_1} \leq & \varepsilon_1 s_1^2 x_1^2 \vartheta_1 + \frac{1}{2} s_1^2 + \frac{1}{2} \mu_1^2(t) s_2^2 + \frac{1}{2} s_1^2 + \frac{1}{2} \mu_1^2(t) X_2^2 \\ & + \mu_1(t) s_1 \alpha_1 + \varepsilon_1 s_1^2 \rho_1 \varrho_1^T \phi_1(\bar{x}_1) + \varepsilon_1 s_1^2 \bar{d}_1 \\ & + s_1 \lambda_1(t) h_1 \left(\overline{\lambda_1^{-1}(t - \tau_1) x_{\bar{\tau}_1}} \right) + \frac{3}{4\varepsilon_1} \end{aligned} \quad (20)$$

where $\bar{d}_1 = \sup ((\lambda_1(t) d_1(t))^2 + \rho_1 \epsilon_{M_1})$.

Now, leveraging Lemma 1, we consider the inequality $\left| h_1 \left(\overline{\lambda_1^{-1}(t - \tau_1) x_{\bar{\tau}_1}} \right) \right| \leq \omega_1 \left(\overline{\lambda_1^{-1}(t - \tau_1)} \right) \Psi_1(\bar{x}_{\bar{\tau}_1})$ where $\overline{\lambda_1^{-1}(t - \tau_1)} = \left[\lambda_1^{-1}(t - \tau_1) \right]^T$ and $\bar{x}_{\bar{\tau}_1} = [x_1(t - \tau_1)]^T$. By using this inequality and Young's inequality, (20) can be expressed as

$$\begin{aligned} \dot{V}_{s_1} \leq & \varepsilon_1 s_1^2 x_1^2 \vartheta_1 + s_1^2 + \frac{1}{2} \mu_1^2(t) s_2^2 + \frac{1}{2} \mu_1^2(t) X_2^2 + \mu_1(t) s_1 \alpha_1 \\ & + \varepsilon_1 s_1^2 \rho_1 \varrho_1^T \phi_1(\bar{x}_1) + \frac{1}{2} s_1^2 \lambda_1^2(t) \omega_1^2 \left(\overline{\lambda_1^{-1}(t - \tau_1)} \right) e^{\beta_1 \bar{\tau}_1} \\ & + \frac{1}{2} e^{-\beta_1 \bar{\tau}_1} \Psi_1^2(\bar{x}_{\bar{\tau}_1}) + \varepsilon_1 s_1^2 \bar{d}_1 + \frac{3}{4\varepsilon_1}. \end{aligned} \quad (21)$$

where β_1 is a positive constant. Since the function Ψ depends on state delays which are unknown, it should be removed from (21). Hence, a positive semi-definite function

$$V_{U_1} = \frac{1}{2(1 - \kappa_1)} \int_{t - \tau_1(t)}^t e^{\beta_1(\xi - t)} \Psi_1^2(\bar{x}_1(\xi)) d\xi \quad (22)$$

is introduced. By differentiating this function with respect to time (t) , the inequality

$$\begin{aligned} \dot{V}_{U_1} = & \frac{1}{2(1 - \kappa_1)} \Psi_1^2(\bar{x}_1(t)) - \beta_1 V_{U_1} \\ & - \frac{1 - \dot{\tau}_1}{2(1 - \kappa_1)} e^{-\beta_1 \tau_1(t)} \Psi_1^2(\bar{x}_{\bar{\tau}_1}) \\ \leq & \frac{1}{2(1 - \kappa_1)} \Psi_1^2(\bar{x}_1(t)) - \frac{1}{2} e^{-\beta_1 \bar{\tau}_1} \Psi_1^2(\bar{x}_{\bar{\tau}_1}) - \beta_1 V_{U_1} \end{aligned} \quad (23)$$

is derived. By adding this equation to (21), we obtain the inequality

$$\begin{aligned} \dot{V}_{s_1} + \dot{V}_{U_1} \leq & \varepsilon_1 s_1^2 x_1^2 \vartheta_1 + s_1^2 + \frac{1}{2} \mu_1^2(t) s_2^2 + \frac{1}{2} \mu_1^2(t) X_2^2 \\ & + \mu_1(t) s_1 \alpha_1 + \varepsilon_1 s_1^2 \rho_1 \varrho_1^T \phi_1(\bar{x}_1) + \varepsilon_1 s_1^2 \bar{d}_1 \\ & + \frac{1}{2(1 - \kappa_1)} \Psi_1^2(\bar{x}_1(t)) - \beta_1 V_{U_1} + \frac{3}{4\varepsilon_1} \\ & + \frac{1}{2} s_1^2 \lambda_1^2(t) \omega_1^2 \left(\overline{\lambda_1^{-1}(t - \tau_1)} \right) e^{\beta_1 \bar{\tau}_1}. \end{aligned} \quad (24)$$

The function $\omega_1^2 \left(\overline{\lambda_1^{-1}(t - \tau_1)} \right)$ is positive and continuous in which $\overline{\lambda_1^{-1}(t - \tau_1)}$ contains bounded elements and $\lambda_1^2(t)$ is a bounded signal. Therefore, there exists a constant positive value $\bar{\omega}_1$ such that $\lambda_1^2(t) \omega_1^2 \left(\overline{\lambda_1^{-1}(t - \tau_1)} \right) \leq \bar{\omega}_1$. Additionally, $\Psi_1^2(\bar{x}_1(t))$ is an indeterminate function that should be approximated by RBF neural networks as

$$\Psi_1^2(\bar{x}_1(t)) = \varsigma_1^T v_1(\bar{x}_1) + \bar{\epsilon}_1, \quad (25)$$

where v_1 is a vector of Gaussian functions, ς_1 is a vector of network weights and an unknown vector of coefficients, and $\bar{\epsilon}_1$ is the approximation error of its estimation. As mentioned earlier, for an appropriate number of Gaussian functions in v_1 , the approximation error $\bar{\epsilon}_1$ is bounded. Thus, there exists a positive constant $\bar{\epsilon}_{M_1}$ such that $|\bar{\epsilon}_1| \leq \bar{\epsilon}_{M_1}$. Now, (24) can be rewritten as follows

$$\begin{aligned} \dot{V}_{s_1} + \dot{V}_{U_1} \leq & \varepsilon_1 s_1^2 x_1^2 \vartheta_1 + s_1^2 + \frac{1}{2} \mu_1^2(t) s_2^2 + \frac{1}{2} \mu_1^2(t) X_2^2 \\ & + \mu_1(t) s_1 \alpha_1 + \varepsilon_1 s_1^2 \rho_1 \varrho_1^T \phi_1(\bar{x}_1) \\ & + \frac{1}{2} s_1^2 e^{\beta_1 \bar{\tau}_1} \bar{\omega}_1 + \frac{1}{2(1 - \kappa_1)} (\varsigma_1^T v(\bar{x}_1)) \\ & + \frac{1}{2(1 - \kappa_1)} \bar{\epsilon}_{M_1} + \varepsilon_1 s_1^2 \bar{d}_1 - \beta_1 V_{U_1} + \frac{3}{4\varepsilon_1}. \end{aligned} \quad (26)$$

The parameters vector and function vector for the first subsystem are defined as

$$\theta_1 = \left[\vartheta_1, \rho_1 \varrho_1^T, \frac{1}{2} e^{\beta_1 \bar{\tau}_1} \bar{\omega}_1, \frac{1}{2(1 - \kappa_1)} s_1^T, \frac{1}{2(1 - \kappa_1)} \bar{\epsilon}_{M_1}, \bar{d}_1 \right]^T \quad (27)$$

$$\Upsilon_1 = \left[\varepsilon_1 s_1 x_1^2, \varepsilon_1 s_1 \varrho_1^T(\bar{x}_1), s_1, \frac{1}{s_1} v_1^T(\bar{x}_1), \frac{1}{s_1}, \varepsilon_1 s_1 \right]^T. \quad (28)$$

By this definition, (26) consequently takes the form

$$\begin{aligned} \dot{V}_{s_1} + \dot{V}_{U_1} \leq & s_1^2 + \frac{1}{2} \mu_1^2(t) s_2^2 + \frac{1}{2} \mu_1^2(t) X_2^2 + \mu_1(t) s_1 \alpha_1 \\ & + (\theta_1^T \Upsilon_1) s_1 - \beta_1 V_{U_1} + \frac{3}{4\varepsilon_1}. \end{aligned} \quad (29)$$

Now, the general positive semi-definite function for the first subsystem is given by

$$V_1 = V_{s_1} + V_{U_1} + \frac{\tilde{\theta}_1^T \Gamma_1^{-1} \tilde{\theta}_1}{2}. \quad (30)$$

Note that $\tilde{\theta}_1 = \hat{\theta}_1 - \theta_1$ and $\Gamma_1 = \Gamma_1^T > 0$ is a matrix to be designed. Also, $\hat{\theta}_1$ is the estimated value of the first subsystem's parameters. Since θ_1 elements are fixed, the derivative of $\hat{\theta}_1$ equals the derivative of the estimated parameters. By differentiating V_1 , the inequality

$$\begin{aligned} \dot{V}_1 \leq & s_1^2 + \frac{1}{2}\mu_1^2(t)s_2^2 + \frac{1}{2}\mu_1^2(t)X_2^2 + \mu_1(t)s_1\alpha_1 \\ & + (\theta_1^T \Upsilon_1)s_1 + \tilde{\theta}_1^T \Gamma_1^{-1} \dot{\tilde{\theta}}_1 - \beta_1 V_{U_1} + \frac{3}{4\varepsilon_1} \end{aligned} \quad (31)$$

is achieved.

Now, the virtual controller α_1 is designed based on (31), which depends on the vector Υ_1 for estimating unknown parameters. However, in (28), elements of the function vector Υ_1 contain s_1 in their denominator, posing a challenge at $s_1 = 0$. To overcome this, α_1 is designed by incorporating the function $q_1(s_1)$ as defined in Lemma 4. α_1 is designed as

$$\begin{cases} \alpha_1 = N(\chi_1)q_1(s_1)[k_1s_1 + \hat{\theta}_1^T \Upsilon_1], \\ \dot{\chi}_1 = q_1(s_1)[k_1s_1^2 + \hat{\theta}_1^T \Upsilon_1s_1], \end{cases} \quad (32)$$

where k_1 should be designed to satisfy the condition $k_1 > 1$. Also, the adaptive law or parameter estimation for the first subsystem is designed as

$$\dot{\tilde{\theta}}_1 = \hat{\dot{\theta}}_1 = q_1(s_1)\Gamma_1 \left(\Upsilon_1s_1 - \sigma_1\hat{\theta}_1 \right) \quad (33)$$

where the constant $\sigma_1 > 0$ and matrix Γ_1 are design parameters.

Remark 3: In (12), $q_i(s_i), i = 1, \dots, n$, shows a decreasing trend for $\delta_{a_i} < |s_i| < \delta_{a_i} + \delta_{b_i}$ and since $|s_i| < \delta_{a_i}$, $q_i(s_i)$ becomes zero. For the first subsystem, this results in $q_1(s_1)$ decreasing to zero before the signal s_1 tends to zero, which resolves the problem at $s_1 = 0$. This solution extends to subsequent subsystem designs.

step i ($i = 2, \dots, n - 1$): By considering (13), the dynamics of the i -th error surface is $\dot{s}_i = \dot{x}_i - \dot{z}_i$, which according to the system (5), can be rewritten as

$$\begin{aligned} \dot{s}_i = & \dot{\lambda}_i(t)\lambda_i^{-1}(t)x_i + \mu_i(t)x_{i+1} + \lambda_i(t)f_i \left(\lambda_i^{-1}(t)x_i \right) \\ & + \lambda_i(t)h_i \left(\lambda_i^{-1}(t - \tau_i)x_{\bar{\tau}_i} \right) + \lambda_i(t)d_i(t) - \dot{z}_i. \end{aligned} \quad (34)$$

The non-negative function $V_{s_i} = \frac{1}{2}s_i^2$ is considered for the i -th subsystem. Its derivative with respect to time, after replacing $x_{i+1} = s_{i+1} + X_{i+1} + \alpha_i$ and using the inequality $ab \leq \varepsilon a^2b^2 + \frac{1}{4\varepsilon}$, is

$$\begin{aligned} \dot{V}_{s_i} = & s_i\dot{s}_i \leq \varepsilon_i s_i^2 x_i^2 \left(\dot{\lambda}_i(t)\lambda_i^{-1}(t) \right)^2 + \varepsilon_i s_i^2 \lambda_i^2(t) f_i^2 \left(\lambda_i^{-1}(t)x_i \right) \\ & + \mu_i(t)s_i (s_{i+1} + X_{i+1} + \alpha_i) + \varepsilon_i s_i^2 \lambda_i^2(t) d_i^2(t) \\ & + s_i \lambda_i(t) h_i \left(\lambda_i^{-1}(t - \tau_i)x_{\bar{\tau}_i} \right) - s_i \dot{z}_i + \frac{3}{4\varepsilon_i}. \end{aligned} \quad (35)$$

Subsequently, the function f_i is estimated utilizing RBF neural networks, similar to the first step as outlined in (19).

Therefore, after using equation (18), we add and subtract the term $\frac{1}{2}\mu_{i-1}^2(t)s_i^2$ to (35) and it transforms to

$$\begin{aligned} \dot{V}_{s_i} \leq & \varepsilon_i s_i^2 x_i^2 \vartheta_i + \frac{1}{2}s_i^2 + \frac{1}{2}\mu_i^2(t)s_{i+1}^2 + \frac{1}{2}s_i^2 + \frac{1}{2}\mu_i^2(t)X_{i+1}^2 \\ & + \mu_i(t)s_i\alpha_i + \varepsilon_i s_i^2 \rho_i \varrho_i^T \phi_i(\bar{x}_i) + \varepsilon_i s_i^2 \bar{d}_i - \frac{1}{2}\mu_{i-1}^2(t)s_i^2 \\ & + s_i \lambda_i(t) h_i \left(\lambda_i^{-1}(t - \tau_i)x_{\bar{\tau}_i} \right) - s_i \dot{z}_i + \frac{3}{4\varepsilon_i} \end{aligned} \quad (36)$$

where $\bar{d}_i = \sup \left((\lambda_i(t)d_i(t))^2 + \frac{1}{2\varepsilon_i}(\mu_{i-1}(t))^2 + \rho_i \varepsilon_{M_i} \right)$.

Remark 4: As evident in (36), the term $\frac{1}{2}\mu_i^2(t)s_{i+1}^2$ is not removable, and the parameter $\mu_i^2(t)$ cannot be estimated within this subsystem due to the appearance of the signal s_{i+1} . This parameter must be estimated in the subsequent step where s_{i+1} is available. Also, for the $(i - 1)$ -th subsystem, the term $\frac{1}{2}\mu_{i-1}^2(t)s_i^2$ appears which its parameter can be estimated in the i -th subsystem. Additionally, due to the use of specific even functions in adaptive laws and virtual controllers, and the challenges in stability analysis, adding subsystems together is not a proper solution. However, adding and subtracting these terms to the subsequent subsystems is an efficient approach.

Now, considering the function $h_i \left(\lambda_i^{-1}(t - \tau_i)x_{\bar{\tau}_i} \right)$, it depends on the states x_1 to x_i and the delays τ_1 to τ_i . Thus, by applying Lemma 2 and subsequently Lemma 1, the inequality

$$\begin{aligned} |h_i \left(\lambda_i^{-1}(t - \tau_i)x_{\bar{\tau}_i} \right)| & \leq \sum_{l=1}^i \Xi_{i,l} \left(\lambda_l^{-1}(t - \tau_l(t))x_l(t - \tau_l(t)) \right) \\ & \leq \sum_{l=1}^i \varpi_{i,l} \left(\lambda_l^{-1}(t - \tau_l) \right) \Psi_{i,l} \left(x_{\tau_l} \right) \end{aligned} \quad (37)$$

is achieved, where $x_{\tau_l} = x_l(t - \tau_l(t))$. Now, using this inequality and Young's inequality, (36) can be written as

$$\begin{aligned} \dot{V}_{s_i} \leq & \varepsilon_i s_i^2 x_i^2 \vartheta_i + s_i^2 + \frac{1}{2}\mu_i^2(t)s_{i+1}^2 + \frac{1}{2}\mu_i^2(t)X_{i+1}^2 \\ & + \mu_i(t)s_i\alpha_i + \varepsilon_i s_i^2 \rho_i \varrho_i^T \phi_i(\bar{x}_i) + \frac{1}{2} \sum_{l=1}^i e^{-\beta_i \bar{\tau}_l} \Psi_{i,l}^2 \left(x_{\tau_l} \right) \\ & + \frac{1}{2}s_i^2 \lambda_i^2(t) \sum_{l=1}^i \varpi_{i,l}^2 \left(\lambda_l^{-1}(t - \tau_l) \right) e^{\beta_i \bar{\tau}_l} + \varepsilon_i s_i^2 \bar{d}_i \\ & - \frac{1}{2}\mu_{i-1}^2(t)s_i^2 - s_i \dot{z}_i + \frac{3}{4\varepsilon_i} \end{aligned} \quad (38)$$

where β_i is a positive constant. Since the function Ψ depends on unknown delays, it should be removed from (38). Hence, a positive semi-definite function

$$V_{U_i} = \sum_{l=1}^i \frac{1}{2(1 - \kappa_l)} \int_{t-\tau_l(t)}^t e^{\beta_i(\xi-t)} \Psi_{i,l}^2(x_l(\xi)) d\xi \quad (39)$$

is introduced. By differentiating this function with respect to time, the inequality

$$\begin{aligned} \dot{V}_{U_i} \leq & \sum_{l=1}^i \frac{1}{2(1-\kappa_l)} \Psi_{i,l}^2(x_l(t)) \\ & - \frac{1}{2} \sum_{l=1}^i e^{-\beta_i \tilde{\tau}_i} \Psi_{i,l}^2(x_{\tau_l}) - \beta_i V_{U_i} \end{aligned} \quad (40)$$

emerges. By adding (40) to (38), we obtain the inequality

$$\begin{aligned} \dot{V}_{s_i} + \dot{V}_{U_i} \leq & \varepsilon_i s_i^2 x_i^2 \vartheta_i + s_i^2 + \frac{1}{2} \mu_i^2(t) s_{i+1}^2 + \frac{1}{2} \mu_i^2(t) X_{i+1}^2 \\ & + \varepsilon_i s_i^2 \rho_i \varrho_i^T \phi_i(\bar{x}_i) + \sum_{l=1}^i \frac{1}{2(1-\kappa_l)} \Psi_{i,l}^2(x_l(t)) \\ & + \frac{1}{2} s_i^2 \lambda_i^2(t) \sum_{l=1}^i \bar{\omega}_{i,l}^2 \left(\lambda_i^{-1}(t - \tau_l) \right) e^{\beta_i \tilde{\tau}_i} - \beta_i V_{U_i} \\ & + \mu_i(t) s_i \alpha_i + \varepsilon_i s_i^2 \bar{d}_i - \frac{1}{2} \mu_{i-1}^2(t) s_i^2 - s_i \dot{z}_i + \frac{3}{4\varepsilon_i}. \end{aligned} \quad (41)$$

As $\bar{\omega}_{i,l}^2$ is a positive continuous function and $\lambda_i^{-1}(t - \tau_l)$ is bounded, there exists a positive constant value $\bar{\omega}_{i,l}$ such that $\lambda_i^2(t) \bar{\omega}_{i,l}^2 \left(\lambda_i^{-1}(t - \tau_l) \right) \leq \bar{\omega}_{i,l}$. Furthermore, the function $\Psi_{i,l}^2(x_l(t))$ is an indeterminate function and it should be approximated by RBF neural networks as

$$\Psi_{i,l}^2(x_l(t)) = \varsigma_{i,l}^T v_{i,l}(x_l) + \bar{\varepsilon}_{i,l}, \quad (42)$$

where $v_{i,l}$ is a vector of Gaussian functions, $\varsigma_{i,l}$ is a vector of network weights and unknown coefficients, and $\bar{\varepsilon}_{i,l}$ is the approximation error. As mentioned earlier, For a proper number of Gaussian functions, we have a positive constant $\bar{\varepsilon}_{M_{i,l}}$ such that $|\bar{\varepsilon}_{i,l}| \leq \bar{\varepsilon}_{M_{i,l}}$. Now, (41) can be rewritten as

$$\begin{aligned} \dot{V}_{s_i} + \dot{V}_{U_i} \leq & \varepsilon_i s_i^2 x_i^2 \vartheta_i + s_i^2 + \frac{1}{2} \mu_i^2(t) s_{i+1}^2 + \frac{1}{2} \mu_i^2(t) X_{i+1}^2 \\ & + \mu_i(t) s_i \alpha_i + \varepsilon_i s_i^2 \rho_i \varrho_i^T \phi_i(\bar{x}_i) + \frac{1}{2} s_i^2 \sum_{l=1}^i \bar{\omega}_{i,l}^2 e^{\beta_i \tilde{\tau}_i} \\ & + \sum_{l=1}^i \frac{1}{2(1-\kappa_l)} \left(\varsigma_{i,l}^T v_{i,l}(x_l) + \bar{\varepsilon}_{i,l} \right) - s_i \dot{z}_i \\ & + \varepsilon_i s_i^2 \bar{d}_i - \frac{1}{2} \mu_{i-1}^2(t) s_i^2 - \beta_i V_{U_i} + \frac{3}{4\varepsilon_i}. \end{aligned} \quad (43)$$

The parameters vector and function vector for the i -th subsystem are defined as

$$\theta_i = \left[\vartheta_i, \rho_i \varrho_i^T, \frac{1}{2} e^{\beta_i \tilde{\tau}_i} \bar{\omega}_{i,1}, \dots, \frac{1}{2} e^{\beta_i \tilde{\tau}_i} \bar{\omega}_{i,i}, \frac{1}{2(1-\kappa_1)} \varsigma_{i,1}^T, \dots, \frac{1}{2(1-\kappa_i)} \varsigma_{i,i}^T, \frac{1}{2(1-\kappa_1)} \bar{\varepsilon}_{M_{i,1}}, \dots, \frac{1}{2(1-\kappa_i)} \bar{\varepsilon}_{M_{i,i}}, \bar{d}_i \right]^T \quad (44)$$

$$\Upsilon_i = \left[\varepsilon_i s_i x_i^2, \varepsilon_i s_i \phi_i^T(\bar{x}_i), s_i, \dots, s_i, \frac{1}{s_i} v_{i,1}^T(x_1), \dots \right]^T$$

$$\left. , \frac{1}{s_i} v_{i,i}^T(x_i), \frac{1}{s_i}, \dots, \frac{1}{s_i}, \varepsilon_i s_i \right]^T. \quad (45)$$

Therefore, equation (43) becomes

$$\begin{aligned} \dot{V}_{s_i} + \dot{V}_{U_i} \leq & s_i^2 + \frac{1}{2} \mu_i^2(t) s_{i+1}^2 + \frac{1}{2} \mu_i^2(t) X_{i+1}^2 + \mu_i(t) s_i \alpha_i \\ & + (\theta_i^T \Upsilon_i) s_i - \frac{1}{2} \mu_{i-1}^2(t) s_i^2 - s_i \dot{z}_i - \beta_i V_{U_i} + \frac{3}{4\varepsilon_i}. \end{aligned} \quad (46)$$

Now, the general positive semi-definite function for the i -th subsystem would be

$$V_i = V_{s_i} + V_{U_i} + \frac{\tilde{\theta}_i^T \Gamma_i^{-1} \tilde{\theta}_i}{2}, \quad (47)$$

where $\tilde{\theta}_i = \hat{\theta}_i - \theta_i$ and $\Gamma_i = \Gamma_i^T > 0$ is a matrix that needs to be designed. Additionally, $\hat{\theta}_i$ represents the estimated value of the parameters for the i -th subsystem. By differentiating V_i , the inequality

$$\begin{aligned} \dot{V}_i \leq & s_i^2 + \frac{1}{2} \mu_i^2(t) s_{i+1}^2 + \frac{1}{2} \mu_i^2(t) X_{i+1}^2 + \mu_i(t) s_i \alpha_i + (\theta_i^T \Upsilon_i) s_i \\ & + \tilde{\theta}_i^T \Gamma_i^{-1} \dot{\tilde{\theta}}_i - \frac{1}{2} \mu_{i-1}^2(t) s_i^2 - s_i \dot{z}_i - \beta_i V_{U_i} + \frac{3}{4\varepsilon_i} \end{aligned} \quad (48)$$

is obtained.

By using Lemma 4 as in the previous steps, the virtual controller α_i would be designed as

$$\begin{cases} \alpha_i = N(\chi_i) q_i(s_i) [k_i s_i + \hat{\theta}_i^T \Upsilon_i - \dot{z}_i], \\ \dot{\chi}_i = q_i(s_i) [k_i s_i^2 + \hat{\theta}_i^T \Upsilon_i s_i - s_i \dot{z}_i], \end{cases} \quad (49)$$

where k_i should be designed to satisfy the condition $k_i > 1$. The adaptive law or parameter estimation for the i -th subsystem is designed as

$$\dot{\tilde{\theta}}_i = \dot{\hat{\theta}}_i = q_i(s_i) \Gamma_i \left(\Upsilon_i s_i - \sigma_i \tilde{\theta}_i \right) \quad (50)$$

where the constant $\sigma_i > 0$ and matrix Γ_i are design parameters.

step n: For the final step, by considering (13), the dynamics of the n -th error surface is $\dot{s}_n = \dot{x}_n - \dot{z}_n$ which according to the system (5), can be rewritten as

$$\begin{aligned} \dot{s}_n = & \dot{\lambda}_n(t) \lambda_n^{-1}(t) x_n + \mu_n(t) u + \mu_{n+1}(t) + \lambda_n(t) f_n \left(\lambda_n^{-1}(t) x_n \right) \\ & + \lambda_n(t) h_n \left(\lambda_n^{-1}(t - \tau_n) x_{\tau_n} \right) + \lambda_n(t) d_n(t) - \dot{z}_n. \end{aligned} \quad (51)$$

The non-negative function $V_{s_n} = \frac{1}{2} s_n^2$ is considered for the n -th subsystem. Its derivative with respect to time is $\dot{V}_{s_n} = s_n \dot{s}_n$ and as in the previous step it can be rewritten as

$$\begin{aligned} \dot{V}_{s_n} \leq & \varepsilon_n s_n^2 x_n^2 \left(\dot{\lambda}_n(t) \lambda_n^{-1}(t) \right)^2 + \mu_n(t) s_n u \\ & + \varepsilon_n s_n^2 \lambda_n^2(t) f_n \left(\lambda_n^{-1}(t) x_n \right)^2 + s_n \lambda_n(t) h_n \left(\lambda_n^{-1}(t - \tau_n) x_{\tau_n} \right) \\ & + \varepsilon_n s_n^2 \left(\lambda_n(t) d_n(t) + \mu_{n+1}(t) \right)^2 - s_n \dot{z}_n + \frac{3}{4\varepsilon_n}. \end{aligned} \quad (52)$$

Additionally, given the uncertainty of the f_n , it can be estimated using RBF neural networks. By using (18) and adding and subtracting the term $\frac{1}{2}\mu_{n-1}^2(t)s_n^2$ to (52), It can be restated as

$$\begin{aligned} \dot{V}_{s_n} \leq & \varepsilon_n s_n^2 x_n^2 \vartheta_n + \mu_n(t) s_n u + \varepsilon_n s_n^2 \rho_n \varrho_n^T \phi_n(\bar{x}_n) \\ & + s_n \lambda_n(t) h_n \left(\lambda_n^{-1}(t - \tau_n) x_{\tau_n} \right) - s_n \dot{z}_n \\ & + \varepsilon_n s_n^2 \bar{d}_n - \frac{1}{2} \mu_{n-1}^2(t) s_n^2 + \frac{3}{4\varepsilon_n} \end{aligned} \quad (53)$$

and $\bar{d}_n = \sup ((\lambda_n(t) d_n(t) + \mu_{n+1}(t))^2 + \frac{1}{2\varepsilon_n} (\mu_{n-1}(t))^2 + \rho_n \varepsilon M_n)$.

Now, by applying (37) for the n -th subsystem (where $i = n$), and using Young's inequality, (53) can be written as

$$\begin{aligned} \dot{V}_{s_n} \leq & \varepsilon_n s_n^2 x_n^2 \vartheta_n + \mu_n(t) s_n u + \vartheta_n s_n^2 \rho_n \varepsilon_n^T \phi_n(\bar{x}_n) - \frac{1}{2} \mu_{n-1}^2(t) s_n^2 \\ & + \frac{1}{2} s_n^2 \lambda_n^2(t) \sum_{l=1}^n \bar{\omega}_{n,l}^2 \left(\lambda_l^{-1}(t - \tau_l) \right) e^{\beta_n \bar{\tau}_l} + \varepsilon_n s_n^2 \bar{d}_n \\ & + \frac{1}{2} \sum_{l=1}^n e^{-\beta_n \bar{\tau}_l} \Psi_{n,l}^2(x_{\tau_l}) - s_n \dot{z}_n + \frac{3}{4\varepsilon_n}, \end{aligned} \quad (54)$$

where β_n is a positive constant. Subsequently, a positive semi-definite function

$$V_{U_n} = \sum_{l=1}^n \frac{1}{2(1 - \kappa_l)} \int_{t-\tau_l(t)}^t e^{\beta_n(\xi-t)} \Psi_{n,l}^2(x_l(\xi)) d\xi \quad (55)$$

is introduced.

Upon differentiating this function with respect to time and adding it to \dot{V}_{s_n} same as in previous steps, the inequality

$$\begin{aligned} \dot{V}_{s_n} + \dot{V}_{U_n} \leq & \varepsilon_n s_n^2 x_n^2 \vartheta_n + \mu_n(t) s_n u + \varepsilon_n s_n^2 \rho_n \varrho_n^T \phi_n(\bar{x}_n) \\ & + \frac{1}{2} s_n^2 \lambda_n^2(t) \sum_{l=1}^n \bar{\omega}_{n,l}^2 \left(\lambda_l^{-1}(t - \tau_l) \right) e^{\beta_n \bar{\tau}_l} \\ & + \sum_{l=1}^n \frac{1}{2(1 - \kappa_l)} \Psi_{n,l}^2(x_l(t)) + \varepsilon_n s_n^2 \bar{d}_n \\ & - \frac{1}{2} \mu_{n-1}^2(t) s_n^2 - s_n \dot{z}_n - \beta_n V_{U_n} + \frac{3}{4\varepsilon_n}. \end{aligned} \quad (56)$$

is obtained. There exists a positive constant $\bar{\omega}_{n,l}$ such that $\lambda_n^2(t) \bar{\omega}_{n,l}^2 \left(\lambda_l^{-1}(t - \tau_l) \right) \leq \bar{\omega}_{n,l}$ (as proven in the i -th step for i -th subsystem). Additionally, $\Psi_{n,l}^2(x_l(t))$ is an unknown function. By using RBF neural networks and (42) for the n -th subsystem (where $i = n$), in which $\bar{\varepsilon}_{M_{n,l}}$ is an upper bound of the approximation error, (56) can be expressed as

$$\begin{aligned} \dot{V}_{s_n} + \dot{V}_{U_n} \leq & \varepsilon_n s_n^2 x_n^2 \vartheta_n + \mu_n(t) s_n u + \varepsilon_n s_n^2 \rho_n \varrho_n^T \phi_n(\bar{x}_n) \\ & + \sum_{l=1}^n \frac{1}{2(1 - \kappa_l)} (s_{n,l}^T v_{n,l}(x_l) + \bar{\varepsilon}_{n,l}) \\ & + \frac{1}{2} s_n^2 \sum_{l=1}^n \bar{\omega}_{n,l}^2 e^{\beta_n \bar{\tau}_l} - \frac{1}{2} \mu_{n-1}^2(t) s_n^2 \end{aligned}$$

$$+ \varepsilon_n s_n^2 \bar{d}_n - s_n \dot{z}_n - \beta_n V_{U_n} + \frac{3}{4\varepsilon_n}. \quad (57)$$

The parameters vector and function vector for the n -th subsystem are defined as

$$\begin{aligned} \theta_n = & \left[\vartheta_n, \rho_n \varrho_n^T, \frac{1}{2} e^{\beta_n \bar{\tau}_1} \bar{\omega}_{n,1}, \dots, \frac{1}{2} e^{\beta_n \bar{\tau}_n} \bar{\omega}_{n,n}, \frac{1}{2(1 - \kappa_1)} s_{n,1}^T, \right. \\ & \dots, \frac{1}{2(1 - \kappa_n)} s_{n,n}^T, \frac{1}{2(1 - \kappa_1)} \bar{\varepsilon}_{M_{n,1}}, \dots \\ & \left. , \frac{1}{2(1 - \kappa_n)} \bar{\varepsilon}_{M_{n,n}}, \bar{d}_n \right]^T \end{aligned} \quad (58)$$

$$\begin{aligned} \Upsilon_n = & \left[\varepsilon_n s_n x_n^2, \varepsilon_n s_n \varphi_n^T(\bar{x}_n), s_n, \dots, s_n, \frac{1}{s_n} v_{n,1}^T(x_1), \dots \right. \\ & \left. , \frac{1}{s_n} v_{n,n}^T(x_n), \frac{1}{s_n}, \dots, \frac{1}{s_n}, \varepsilon_n s_n \right]^T. \end{aligned} \quad (59)$$

Therefore, (57) can be rewritten as

$$\begin{aligned} \dot{V}_{s_n} + \dot{V}_{U_n} \leq & \mu_n(t) s_n u + (\theta_n^T \Upsilon_n) s_n - \frac{1}{2} \mu_{n-1}^2(t) s_n^2 \\ & - s_n \dot{z}_n - \beta_n V_{U_n} + \frac{3}{4\varepsilon_n}. \end{aligned} \quad (60)$$

Now, the general positive semi-definite function for the n -th subsystem would be

$$V_n = V_{s_n} + V_{U_n} + \frac{\tilde{\theta}_n^T \Gamma_n^{-1} \tilde{\theta}_n}{2}, \quad (61)$$

where $\tilde{\theta}_n = \hat{\theta}_n - \theta_n$ and $\Gamma_n = \Gamma_n^T > 0$ is a matrix to be designed. Additionally, $\hat{\theta}_n$ represents the estimated parameters for the n -th subsystem. By differentiating V_n , the inequality

$$\begin{aligned} \dot{V}_n \leq & \mu_n(t) s_n u + (\theta_n^T \Upsilon_n) s_n + \tilde{\theta}_n^T \Gamma_n^{-1} \dot{\tilde{\theta}}_n - \frac{1}{2} \mu_{n-1}^2(t) s_n^2 \\ & - s_n \dot{z}_n - \beta_n V_{U_n} + \frac{3}{4\varepsilon_n}. \end{aligned} \quad (62)$$

is obtained.

Eventually, the control signal u is designed as

$$\begin{cases} u = N(\chi_n) q_n(s_n) [k_n s_n + \hat{\theta}_n^T \Upsilon_n - \dot{z}_n], \\ \dot{\chi}_n = q_n(s_n) [k_n s_n^2 + \hat{\theta}_n^T \Upsilon_n s_n - s_n \dot{z}_n], \end{cases} \quad (63)$$

where k_n should be designed to satisfy the condition $k_n > 0$. Additionally, the adaptive law or parameter estimation for the n -th subsystem is designed as

$$\dot{\hat{\theta}}_n = \dot{\tilde{\theta}}_n = q_n(s_n) \Gamma_n \left(\Upsilon_n s_n - \sigma_n \hat{\theta}_n \right), \quad (64)$$

where the constant $\sigma_n > 0$ and matrix Γ_n are design parameters.

Now, to better understand, the flowchart in Fig. 2 shows that many theoretical complexities are not involved in the practical process of the controller design. Based on this flowchart, the uncertain parameters of the system, including

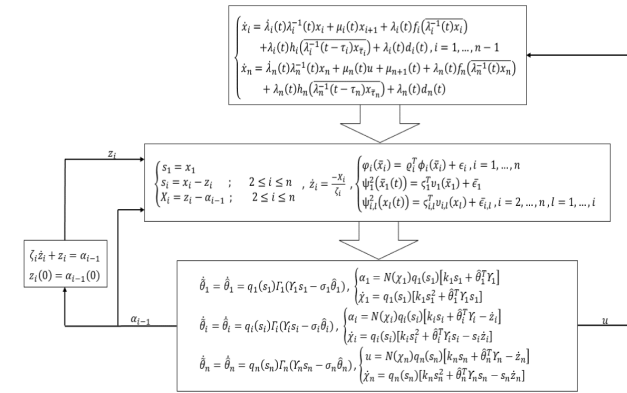


FIGURE 2. The flowchart of the controller design process.

uncertainties in the system itself and those caused by attacks, are estimated using adaptive laws at each step. Consequently, the virtual controllers are designed using these estimated parameters. Finally, the main controller of the system is designed utilizing the virtual controllers and estimated parameters and is applied to the system under attack.

Theorem 1: Consider the system described by (1), which is susceptible to both injection and deception attacks (2). The structure of the controller (63) and the adaptive laws for parameters (33), (50), and (64), in addition to ensuring the boundedness of signals in the closed-loop system, guarantee that over an extended period and in a steady state, the error surface signal vector $s(t) = [s_1, \dots, s_n]^T$ converges to

$$\Lambda_s = \{s \mid \|s\| \leq \Omega\},$$

$$\Omega = \max \left\{ \sqrt{2\left(\frac{D}{C} + B\right)}, \sqrt{\sum_{i=1}^n (\delta_{a_i} + \delta_{b_i})^2} \right\} \quad (65)$$

where D denotes the upper bound of

$$\sum_{i=1}^n \left(\frac{1}{2} \sigma_i \|\theta_i\|^2 + \frac{3}{4(\epsilon_i)} \right) + \sum_{i=1}^{n-1} \left(\frac{1}{2} \mu_i^2(t) X_{i+1}^2 \right),$$

and C is given by $C = \min \{\bar{C}_1, \bar{C}_2, \dots, \bar{C}_n\}$, where $\bar{C}_i = \min \left(\frac{\sigma_i}{\lambda_{\max}(\Gamma_i^{-1})}, 2\bar{k}_i, \beta_i \right)$, $i = 1, \dots, n$. Here, $\bar{k}_i = k_i - 1$ for $i = 1, \dots, n-1$, and $\bar{k}_n = k_n$. The variable B is defined as an upper bound of

$$e^{-Ct} \sum_{i=1}^n \int_0^t \mu_i(t) N(\chi_i) \dot{\chi}_i e^{C\tau} d\tau + e^{-Ct} \sum_{i=1}^n \int_0^t \dot{\chi}_i e^{C\tau} d\tau.$$

Proof: To prove the proposed theorem, two positive semi-definite functions are considered: $V(t) = \sum_{i=1}^n V_i$ and $V_X = \sum_{i=2}^n \frac{1}{2} X_i^2$, where the function V_X undergoes differentiation yielding $\dot{V}_X = \sum_{i=2}^n X_i \dot{X}_i = \sum_{i=2}^n X_i (\dot{z}_i - \dot{\alpha}_{i-1})$. By defining a continuous function $D_i(\cdot) \triangleq -\dot{\alpha}_{i-1}$, it can be expressed as

$$\dot{V}_X = \sum_{i=2}^n X_i \dot{X}_i = \sum_{i=2}^n \frac{-X_i^2}{\zeta_i} + X_i D_i. \quad (66)$$

To prove the boundedness of the functions $D_i(\cdot)$, the compact set Π is defined as

$$\Pi = \left\{ (s_i, X_i, \hat{\theta}_i) \mid \sum_{i=1}^n \frac{1}{2} s_i^2 + \sum_{i=2}^n \frac{1}{2} X_i^2 + \sum_{i=1}^n \frac{1}{2} \hat{\theta}_i^T \hat{\theta}_i \leq P \right\}$$

where P is a positive constant. Given that all types of variables of the function D_i are in this set, according to the Heine-Borel theorem [31], the continuous D_i is bounded on this compact set and there exists a positive constant M_i such that $|D_i(\cdot)| \leq M_i$. For every $\delta_i \geq 0$, the inequality

$$|X_i D_i(\cdot)| \leq \frac{X_i^2 D_i^2}{4\delta_i} + \delta_i \leq \frac{X_i^2 M_i^2}{4\delta_i} + \delta_i$$

holds. Therefore, K_i^* should be designed in such a way that the condition $K_i^* = \frac{1}{\zeta_i} - \frac{M_i^2}{4\delta_i} \geq 0$ is maintained. In this case, (66) takes the form

$$\dot{V}_X \leq -K^* V_X + \delta \quad (67)$$

where, $K^* = \min \{K_2^*, \dots, K_n^*\}$ and $\delta = \sum_{i=2}^n \delta_i$. Now, both sides of (67) are multiplied by e^{K^*t} . By solving this differential inequality, the relation

$$V_X \leq e^{-K^*t} (V_X(0) - \delta) + \delta, \quad (68)$$

is obtained, which implies that V_X and signals $X_i, i = 1, \dots, n$ are bounded. By properly designing $\zeta_i, i = 1, \dots, n$, they can be made as small as desired.

Remark 5: Due to the utilization of the function $q_i(s_i)$ in the design process, the stability proof is divided into three regions. When $q_i(s_i) \neq 1$, considering only one positive function $V = \sum_{i=1}^n V_i + V_X$ allows us to establish the boundedness of s_i , but we cannot prove the boundedness of X_i . Additionally, according to equation (48), due to the existence of μ_i^2 as a coefficient of X_{i+1}^2 , which is produced by attackers, the time constant of the filter (ζ_{i+1}), cannot be appropriately designed. Therefore, employing two positive semi-definite functions instead of a single general positive definite function is a suitable solution to address this issue.

Now, the proof of $V(t)$ is conducted by considering four distinct cases. Firstly, we explore cases where all s_i satisfy $|s_i| \geq \delta_{a_i} + \delta_{b_i}$ or $\delta_{a_i} \leq |s_i| \leq \delta_{a_i} + \delta_{b_i}$ or $|s_i| \leq \delta_{a_i}$. The boundedness of $V(t)$ is examined in each of these cases. Subsequently, we explore a case where the values of s_i differ and are in different ranges.

First case: In this case, where $|s_i| \geq \delta_{a_i} + \delta_{b_i}$ and $q_i(s_i) = 1$ for $i = 1, \dots, n$, the time derivative of $V(t)$ can be expressed as

$$\begin{aligned} \dot{V}(t) \leq & \sum_{i=1}^n s_i^2 + \sum_{i=1}^{n-1} \mu_i^2(t) X_{i+1}^2 + \sum_{i=1}^n \mu_i(t) N(\chi_i) \dot{\chi}_i \\ & + \sum_{i=1}^n (\theta_i^T \Upsilon_i) s_i + \sum_{i=1}^n \tilde{\theta}_i^T \Gamma_i^{-1} \dot{\tilde{\theta}}_i - \sum_{i=2}^n s_i \dot{z}_i \\ & - \sum_{i=1}^n \beta_i V_{U_i} + \sum_{i=1}^n \frac{3}{4\epsilon_i}. \end{aligned} \quad (69)$$

By adding and subtracting $\dot{\chi}_i$ and carefully designing k_i , while applying the adaptive laws (33), (50), and (64), the inequality (69) transforms into

$$\begin{aligned} \dot{V}(t) \leq & -\sum_{i=1}^n \bar{k}_i s_i^2 + \sum_{i=1}^n (\mu_i(t)N(\chi_i) + 1) \dot{\chi}_i - \sum_{i=1}^n \sigma_i \tilde{\theta}_i^T \hat{\theta}_i \\ & - \sum_{i=1}^n \beta_i V_{U_i} + \sum_{i=1}^{n-1} \mu_i^2(t) X_{i+1}^2 + \sum_{i=1}^n \frac{3}{4\varepsilon_i}. \end{aligned} \quad (70)$$

Using $-\sum_{i=1}^n \sigma_i \tilde{\theta}_i^T \hat{\theta}_i \leq \sum_{i=1}^n \frac{1}{2} \sigma_i \|\theta_i\|^2 - \sum_{i=1}^n \frac{1}{2} \sigma_i \|\tilde{\theta}_i\|^2$, we have

$$\dot{V}(t) \leq -CV(t) + \sum_{i=1}^n (\mu_i(t)N(\chi_i) + 1) \dot{\chi}_i + D \quad (71)$$

where C and D have been already defined in Theorem 1. If we multiply both sides by e^{Ct} and integrate it, the inequality

$$\begin{aligned} V(t) \leq & e^{-Ct} \sum_{i=1}^n \int_0^t \mu_i(\tau)N(\chi_i) \dot{\chi}_i e^{C\tau} d\tau \\ & + e^{-Ct} \sum_{i=1}^n \int_0^t \dot{\chi}_i e^{C\tau} d\tau + (V(0) - \frac{D}{C})e^{-Ct} + \frac{D}{C}. \end{aligned} \quad (72)$$

is obtained. Now, by applying lemma 3, the boundedness of $V(t)$ and $\chi_i(t)$ can easily be obtained. By substituting B , as defined in Theorem 1, we have $V(t) \leq B + (V(0) - \frac{D}{C})e^{-Ct} + \frac{D}{C}$. In the steady state, the limit of $V(t)$ is $\lim_{t \rightarrow \infty} V(t) \leq B + \frac{D}{C}$, implying that the limit of $s(t)$ is

$$\lim_{t \rightarrow \infty} \|s(t)\| \leq \sqrt{2 \left(\frac{D}{C} + B \right)}.$$

Second case: In this case, all s_i are confined within the range $\delta_{a_i} \leq |s_i| \leq \delta_{a_i} + \delta_{b_i}$ for $i = 1, \dots, n$. The value of s_i is bounded within this region and due to the boundedness of X_i , the signals x_i , and the functions V_{s_i} and V_{U_i} are also bounded. To establish the stability of the positive semi-definite functions V_i , $i = 1, \dots, n$, it is essential to verify the boundedness of the functions $V_{\theta_i} = \frac{\tilde{\theta}_i^T \Gamma_i^{-1} \tilde{\theta}_i}{2}$. By differentiating it and applying the adaptive laws (50), its derivative is expressed as

$$\dot{V}_{\theta_i} = \tilde{\theta}_i^T \Gamma_i^{-1} \dot{\tilde{\theta}}_i = \tilde{\theta}_i^T q_i(s_i) (\Upsilon_i s_i - \sigma_i \hat{\theta}_i). \quad (73)$$

Utilizing the inequalities

$$\begin{cases} q_i(s_i) \tilde{\theta}_i^T \Upsilon_i s_i \leq \frac{1}{2c'_i} q_i(s_i) \|\tilde{\theta}_i\|^2 + \frac{c'_i}{2} q_i(s_i) \Upsilon_i^T \Upsilon_i s_i^2, & c'_i > 0 \\ -\sigma_i \tilde{\theta}_i^T \hat{\theta}_i \leq -\frac{1}{2} \sigma_i \|\tilde{\theta}_i\|^2 + \frac{1}{2} \sigma_i \|\theta_i\|^2 \end{cases}$$

equation (73) transforms into

$$\begin{aligned} \dot{V}_{\theta_i} \leq & -\frac{1}{2} q_i(s_i) \left(\sigma_i - \frac{1}{c'_i} \right) \|\tilde{\theta}_i\|^2 \\ & + \frac{1}{2} q_i(s_i) \left(\sigma_i \|\theta_i\|^2 + c'_i \Upsilon_i^T \Upsilon_i s_i^2 \right). \end{aligned} \quad (74)$$

In this region, the vector Υ_i consists of functions that are all smooth and bounded. Therefore, with a suitable choice of c'_i such that $\sigma_i - \frac{1}{c'_i} > 0$, the inequality

$$\dot{V}_{\theta_i} \leq -C_{\theta_i}^* V_{\theta_i} + \rho_{\theta_i} \quad (75)$$

is obtained, where the parameters $C_{\theta_i}^* = q_i(s_i) \frac{\sigma_i^*}{\lambda_{\max}(\Gamma_i^{-1})}$ and $\rho_{\theta_i} = \frac{1}{2} q_i(s_i) (\sigma_i \|\theta_i\|^2 + c'_i \Upsilon_i^T \Upsilon_i s_i^2)$. Similar to (67) and (68), the boundedness of the function V_{θ_i} and $\hat{\theta}_i$ for $i = 1, \dots, n$, and ultimately V_i , $i = 1, \dots, n$, is established and all signals of the closed-loop system will be bounded within this region. Additionally, considering $\delta_{a_i} \leq |s_i| \leq \delta_{a_i} + \delta_{b_i}$, $i = 1, \dots, n$, we have $\|s\| \leq \sqrt{\sum_{i=1}^n (\delta_{a_i} + \delta_{b_i})^2}$.

Third case: In this case, all s_i are limited to the interval $|s_i| \leq \delta_{a_i}$ for $i = 1, \dots, n$. As a result, the signals s_i are all bounded in this region. Due to the boundedness of X_i , the signal x_i and the functions V_{s_i} and V_{U_i} are also bounded. Also, since $q_i(s_i) = 0$, $\hat{\theta}_i$, and α_{i-1} for $i = 1, \dots, n$ are equal to zero, this means that $\tilde{\theta}_i$ remains in a limited range and is bounded. Therefore, the functions $V_{\theta_i} = \frac{\tilde{\theta}_i^T \Gamma_i^{-1} \tilde{\theta}_i}{2}$ and V_i are bounded for $i = 1, \dots, n$.

Fourth case: In this case, the signals s_i are in different regions: some are in the region $|s_i| \geq \delta_{a_i} + \delta_{b_i}$, some in $\delta_{a_i} \leq |s_i| \leq \delta_{a_i} + \delta_{b_i}$ or $|s_i| \leq \delta_{a_i}$. For instance, if $|s_i| \geq \delta_{a_i} + \delta_{b_i}$ and $|s_{i+1}| \leq \delta_{a_{i+1}}$ or $\delta_{a_{i+1}} \leq |s_{i+1}| \leq \delta_{a_{i+1}} + \delta_{b_{i+1}}$, we conclude that all signals in the $(i + 1)$ -th subsystem are bounded, similar to the proof in the second and third case. To prove the boundedness of the signals in the i -th subsystem, if we replace (49) and (50) in (48) we realize that its stability depends on s_{i+1} which is bounded. This implies that the signals in the i -th subsystem are also bounded. Additionally, the n -th subsystem is bounded when $|s_n| \geq \delta_{a_n} + \delta_{b_n}$ and doesn't depend on other subsystems.

In summary, the proof covers all possible scenarios, demonstrating that all signals of the closed-loop system are bounded, and the signal $s(t) = [s_1, \dots, s_n]^T$ converges over time to the region Ω .

IV. SIMULATION AND EXAMPLES

In this section, we simulate two examples to demonstrate the effectiveness and performance of the proposed method and controller. We present the results to evaluate the method's capabilities.

Example 1. Consider the system

$$\begin{cases} \dot{\tilde{x}}_1 = g_1(t) \tilde{x}_2 + f_1(\tilde{x}_1) + h_1(\tilde{x}_{\tau_1}) + d_1(t) \\ \dot{\tilde{x}}_2 = g_2(t) \tilde{u} + f_2(\tilde{x}_2) + h_2(\tilde{x}_{\tau_2}) + d_2(t) \end{cases} \quad (76)$$

where $g_1(t) = 1 + 0.5 \sin(t)$, $g_2(t) = -3 + \cos^2(t)$, $d_1(t) = 0.05 + 0.02 \cos(t)$, and $d_2(t) = 0.05$ are unknown. Additionally, $f_1(\tilde{x}_1) = (-2 + 0.2 \cos(t)) \tilde{x}_1^2 e^{\tilde{x}_1} + \sin(t) \tilde{x}_1 \cos(\tilde{x}_1)$, $h_1(\tilde{x}_{\tau_1}) = (2 + \sin^2(t)) \tilde{x}_1^2 (t - \tau_1(t))$, $f_2(\tilde{x}_2) = (1.5 + 0.5 \tanh(t)) \tilde{x}_1 \tilde{x}_2 + (2 + \cos^2(t)) \tilde{x}_2 \cos(\tilde{x}_1)$, $h_2(\tilde{x}_{\tau_2}) = \tilde{x}_2^2 (t - \tau_2(t)) \sin(\tilde{x}_1 (t - \tau_1(1)))$ where $\tau_1(t) = 1.2 + 0.3 \cos^2(t)$ and

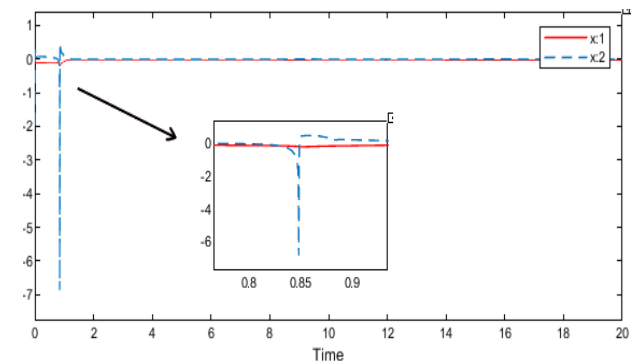


FIGURE 3. The true system states in Example 1 under the first scenario attack which are not accessible.

$\tau_2(t) = 0.8 + 0.2 \sin(t)$. Functions f_1, f_2, h_1 , and h_2 are all unknown.

The controller design parameters are also as follows: $\delta_{a1} = \delta_{b1} = 0.1, \delta_{a2} = \delta_{b2} = 0.1, \epsilon_1 = \epsilon_2 = 0.1, k_1 = 2, k_2 = 3, \sigma_1 = \sigma_2 = 0.001, \zeta_2 = 0.01$, and Γ_1 and Γ_2 are diagonal matrices with diagonal elements of 1. The initial states of the system are considered as $x_1(0) = -0.1$ and $x_2(0) = -0.2$ and the Nussbaum function is used as $N(\chi) = \cosh(\alpha\chi) \sin(\chi/\beta)$ where $\alpha = 0.4$ and $\beta = 0.3$. In this example, considering that the functions f_1, f_2, h_1 , and h_2 are unknown, RBF neural networks have been used to estimate them.

Remark 6: In the process of designing the controller, functions f_i are not directly estimated, because their variable is the product of λ_i which is introduced by attackers and false states. Consequently, we focus on estimating functions φ_i that solely depend on the false states. Therefore, we can consider f_i similar to example 1 in which some bounded time-varying parameters exist. These parameters along with other time-varying attack parameters, λ_i , can be isolated using Lemma 1.

To assess the proposed method, we explore its effectiveness in two distinct attack scenarios.

Scenario 1: In this scenario, we assume that the system experiences continuous attacks from the outset. The attack parameters are defined as $w_1(t) = -5 + \sin^2(t), w_2(t) = 3 + \tan^{-1}(t), b(t) = 3 + 2 \sin(t) \cos(t)$, and also $v(t) = 8$. The results of this attack scenario are illustrated in Fig. 3 and Fig. 4.

Scenario 2: For this scenario, we assume that attacks occur at $t = 20$. The attack parameters for this scenario are specified as $w_1(t) = 7 + \sin(t) \cos(t), w_2(t) = -6 - \cos^2(0.2t), b(t) = -4 - \sin^2(t)$, and $v(t) = 5 + 3 \tanh(t)$. The corresponding results for this attack scenario can be observed in Fig. 5 and Fig. 6.

Fig. 3 illustrates the system's true states in the first scenario. Although the system's dynamics are complicated, the signals show an approximately favorable transient behavior with acceptable speed and overshoot. Fig. 4 displays the input signal in this scenario as applied to the system. Due to the impact of attacks and inherent complexities of the system, the signal exhibits a large fluctuation range in its transient

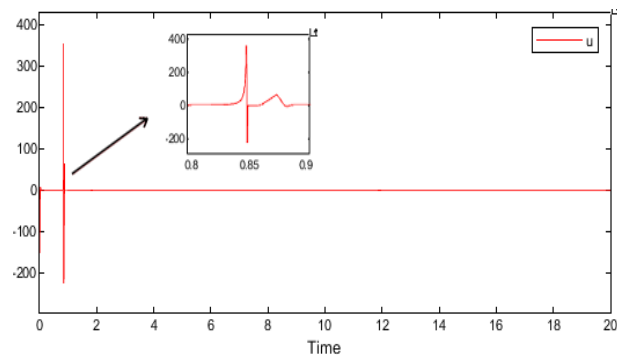


FIGURE 4. The system input in Example 1, which has been affected by deception attacks under the first scenario.

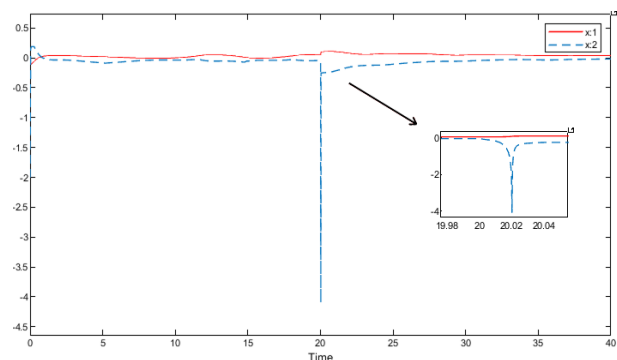


FIGURE 5. The true system states in Example 1 under the second scenario attack which are not accessible.

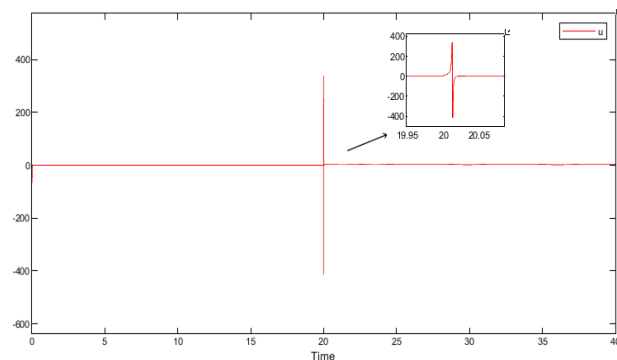


FIGURE 6. The system input in Example 1, which has been affected by deception attacks under the second scenario.

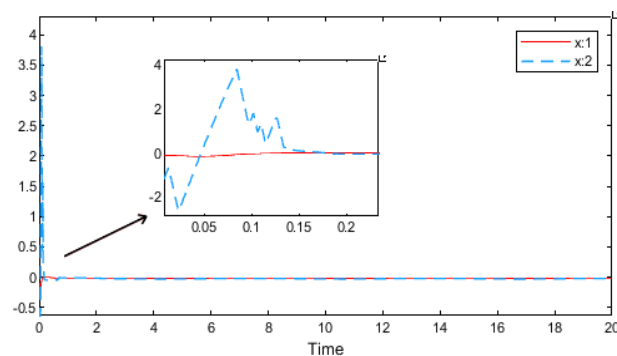


FIGURE 7. The true system states in Example 2 under the first scenario attack which are not accessible.

behavior. In Fig. 5, the system's true states in the second scenario are shown. Initially, they quickly converge to the

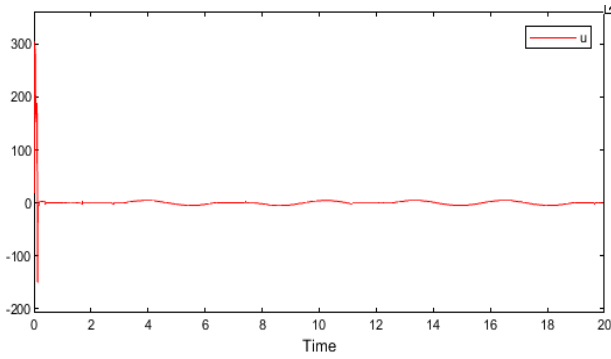


FIGURE 8. The system input in Example 2, which has been affected by deception attacks under the first scenario.

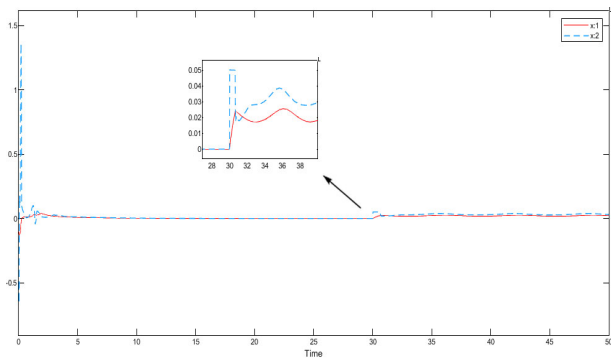


FIGURE 9. The true system states in Example 2 under the second scenario attack which are not accessible.

origin with a transient behavior. At $t = 20$, they exhibit another favorable transient behavior due to the attacks and subsequently, there's another convergence to a neighborhood around the origin. Fig. 6 shows the input signal in the second scenario. Initially, it is equal to the designed control signal before the attack. After the attacks, the signal stabilizes again with a transient response.

Example 2. In this example, we simulate a nonlinear time-delay practical system, By considering the 2nd order chemical reactor system described as

$$\begin{cases} \dot{\tilde{x}}_1 &= -(C_1 + \frac{1}{R_1})\tilde{x}_1 - \frac{1}{R_1}\tilde{x}_1(t - \tau_1(t)) + \frac{1 - F_2}{B_1}\tilde{x}_2 \\ \dot{\tilde{x}}_2 &= -C_2\tilde{x}_2 - \frac{1}{R_2}\tilde{x}_2^2 - \frac{2E_2}{R_2}\tilde{x}_2 + \frac{F_1}{B_2}\tilde{x}_1(t - \tau_1(t)) \\ &+ \frac{F_2}{B_2}\tilde{x}_2(t - \tau_2(t)) + \frac{F_r}{B_2}\tilde{u} \end{cases} \quad (77)$$

where, $C_1 = C_2 = 0.5$, $R_1 = R_2 = 2$, $B_1 = B_2 = 0.5$, $F_1 = F_2 = 0.5$, $E_2 = \frac{7}{3}$, and $F_r = 0.5$, following the considerations in [19]. The time delays are introduced as $\tau_1(t) = 0.5(2.5 + \sin(t))$ and $\tau_2(t) = 0.5(3 + 0.4 \cos(2t))$ which are also unknown. Notably, the initial states of the system are given by $x_1(0) = -0.1$ and $x_2(0) = -0.5$.

The controller is designed with specific parameters: $\varepsilon_1 = \varepsilon_2 = 0.1$, $k_1 = 2$, $k_2 = 2$, $\sigma_1 = \sigma_2 = 0.001$, $\delta_{a_1} = \delta_{b_1} = 0.1$, $\delta_{a_2} = \delta_{b_2} = 0.1$, $\zeta_2 = 0.01$, and Γ_1, Γ_2 are diagonal matrices with diagonal elements set to 0.1. Moreover, the Nussbaum function used in this context is $N(\chi) = \cosh(\alpha\chi) \sin(\chi/\beta)$

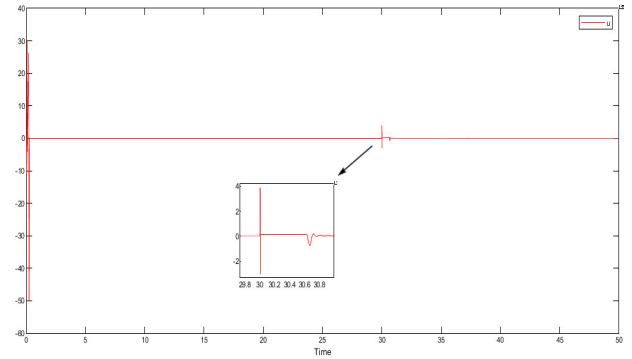


FIGURE 10. The system input in Example 2, which has been affected by deception attacks under the second scenario.

where $\alpha = 0.3$ and $\beta = 1$. For the estimation of unknown functions of the system, RBF neural networks have been employed.

To evaluate the proposed method, we examine its efficacy in two different attack scenarios.

Scenario 1: In this scenario, we assume that the system experiences continuous attacks from the beginning. The attack parameters are defined as $w_1(t) = -5 - \sin(t) + 2 \tanh(t)$, $w_2(t) = 3 + 2 \sin(t) \cos(t)$, $b(t) = 4 + \cos(t)$, and also $v(t) = 10 \sin(t) \cos(t)$. The results of this attack scenario are illustrated in Fig. 7 and Fig. 8.

Scenario 2: For this particular scenario, we consider that attacks occur at $t = 30$. The attack parameters for this scenario are specified as $w_1(t) = 4 + \sin(t)$, $w_2(t) = -3 - 0.2 \cos(t)$, $b(t) = -3$, and $v(t) = 4 + \sin(t) \cos(t)$. The corresponding results for this attack scenario can be observed in Fig. 9 and Fig. 10.

Fig. 7 shows the system's true states under the first scenario attack, exhibiting a favorable transient behavior with acceptable speed and overshoot. In Fig. 8, the input signal applied to the system under the first attack scenario is displayed. Due to the impact of unknown delays in the states and the attack parameters including more than one frequency, the transient response shows large variations. Notably, the range of these fluctuations is due to the impact of deception attacks on the system. In Fig. 9, the true system's states with the second scenario attack converge approximately to the origin within a settling time of less than 3 seconds from the system's start. At $t = 30$, they exhibit another transient behavior, converging to a neighborhood around the origin with favorable variations. Fig. 10 depicts the input signal under the second scenario attack, applied to the system. Before the attack, it equals the control signal sent from the controller. During the attack, the signal changes but stabilizes with a favorable transient state.

V. CONCLUSION

In this paper, the design of a controller for uncertain nonlinear time-delay CPSs under injection and deception attacks was investigated. We applied a series of even functions to address the issue of zeroing signals in the controller's denominator without imposing any additional conditions or restrictions

on the system. The utilization of these functions posed some challenges in the dynamic surface method. Therefore, we addressed these challenges in our study and successfully resolved them. We demonstrated that the designed controller guarantees the boundedness of the system's closed-loop signals. Finally, to assess the effectiveness of the proposed method, we presented two simulation examples and evaluated their outcomes. Possible future works include considering time delays in attack modeling for nonlinear time-delay CPSs.

REFERENCES

- [1] J. Shi, J. Wan, H. Yan, and H. Suo, "A survey of cyber-physical systems," in *Proc. Int. Conf. Wireless Commun. Signal Process. (WCSP)*, Nov. 2011, pp. 1–6.
- [2] Y. Liu, Y. Peng, B. Wang, S. Yao, and Z. Liu, "Review on cyber-physical systems," *IEEE/CAA J. Autom. Sinica*, vol. 4, no. 1, pp. 27–40, Jan. 2017.
- [3] C. Neuman, "Challenges in security for cyber-physical systems," *Work. Futur. Dir. Cyber-Physical Syst. Secur.*, pp. 1–4, 2009.
- [4] Y. Ashibani and Q. H. Mahmoud, "Cyber physical systems security: Analysis, challenges and solutions," *Comput. Secur.*, vol. 68, pp. 81–97, Jul. 2017.
- [5] M. S. Mahmoud, M. M. Hamdan, and U. A. Baroudi, "Modeling and control of cyber-physical systems subject to cyber attacks: A survey of recent advances and challenges," *Neurocomputing*, vol. 338, pp. 101–115, Apr. 2019.
- [6] P. Antsaklis, "Goals and challenges in cyber-physical systems research editorial of the editor in chief," *IEEE Trans. Autom. Control*, vol. 59, no. 12, pp. 3117–3119, Dec. 2014.
- [7] S. Feng and P. Tesi, "Resilient control under denial-of-service: Robust design," *Automatica*, vol. 79, pp. 42–51, May 2017.
- [8] Z. Zuo, X. Cao, Y. Wang, and W. Zhang, "Resilient consensus of multiagent systems against denial-of-service attacks," *IEEE Trans. Syst. Man, Cybern. Syst.*, vol. 52, no. 4, pp. 2664–2675, Apr. 2022.
- [9] C. De Persis and P. Tesi, "Input-to-state stabilizing control under denial-of-service," *IEEE Trans. Autom. Control*, vol. 60, no. 11, pp. 2930–2944, Nov. 2015.
- [10] C. Beck and P. Viswanath, in *Proc. 47th Annu. Allerton Conf. Commun., Control, Comput.*, 2009, pp. 911–918.
- [11] M. Zhu and S. Martínez, "On the performance analysis of resilient networked control systems under replay attacks," *IEEE Trans. Autom. Control*, vol. 59, no. 3, pp. 804–808, Mar. 2014.
- [12] M. Yadegar, N. Meskin, and W. M. Haddad, "An output-feedback adaptive control architecture for mitigating actuator attacks in cyber-physical systems," *Int. J. Adapt. Control Signal Process.*, vol. 33, no. 6, pp. 943–955, Jun. 2019.
- [13] T. Yucelen, W. M. Haddad, and E. M. Feron, "Adaptive control architectures for mitigating sensor attacks in cyber-physical systems," *Cyber-Phys. Syst.*, vol. 2, nos. 1–4, pp. 24–52, Oct. 2016.
- [14] X. Jin, W. M. Haddad, and T. Yucelen, "An adaptive control architecture for mitigating sensor and actuator attacks in cyber-physical systems," *IEEE Trans. Autom. Control*, vol. 62, no. 11, pp. 6058–6064, Nov. 2017.
- [15] X. Ren and G. Yang, "Adaptive control for nonlinear cyber-physical systems under false data injection attacks through sensor networks," *Int. J. Robust Nonlinear Control*, vol. 30, no. 1, pp. 65–79, Jan. 2020.
- [16] Y. Yang, J. Huang, X. Su, and B. Deng, "Adaptive control of cyber-physical systems under deception and injection attacks," *J. Franklin Inst.*, vol. 358, no. 12, pp. 6174–6194, Aug. 2021.
- [17] Y. Yang, J. Huang, X. Su, K. Wang, and G. Li, "Adaptive control of second-order nonlinear systems with injection and deception attacks," *IEEE Trans. Syst. Man, Cybern. Syst.*, vol. 52, no. 1, pp. 574–581, Jan. 2022.
- [18] Q. Zhang and D. He, "Adaptive neural control of nonlinear cyber-physical systems against randomly occurring false data injection attacks," *IEEE Trans. Syst. Man, Cybern. Syst.*, vol. 53, no. 4, pp. 2444–2455, Apr. 2023.
- [19] S. J. Yoo, "Neural-Network-Based adaptive resilient dynamic surface control against unknown deception attacks of uncertain nonlinear time-delay cyberphysical systems," *IEEE Trans. Neural Netw. Learn. Syst.*, vol. 31, no. 10, pp. 4341–4353, Oct. 2020.
- [20] S. Song, J. H. Park, B. Zhang, and X. Song, "Adaptive NN finite-time resilient control for nonlinear time-delay systems with unknown false data injection and actuator faults," *IEEE Trans. Neural Netw. Learn. Syst.*, vol. 33, no. 10, pp. 5416–5428, Oct. 2022.
- [21] Z. Chen, "Nussbaum functions in adaptive control with time-varying unknown control coefficients," *Automatica*, vol. 102, pp. 72–79, Apr. 2019.
- [22] H. Sun, Y. Cui, L. Hou, and K. Shi, "Adaptive finite-time control for cyber-physical systems with injection and deception attacks," *Appl. Math. Comput.*, vol. 430, Oct. 2022, Art. no. 127316.
- [23] A. Nemati, M. Peimani, S. Mobayen, and S. Sayyedfatahi, "Adaptive non-singular finite time control of nonlinear disturbed cyber-physical systems with actuator cyber-attacks and time-varying delays," *Inf. Sci.*, vol. 612, pp. 1111–1126, Oct. 2022.
- [24] B. Miao, H. Wang, Y.-J. Liu, and L. Liu, "Adaptive security control against false data injection attacks in cyber-physical systems," *IEEE J. Emerg. Sel. Topics Circuits Syst.*, vol. 13, no. 3, pp. 743–751, Aug. 2023.
- [25] H. Wang, W. Sun, and P. X. Liu, "Adaptive intelligent control of nonaffine nonlinear time-delay systems with dynamic uncertainties," *IEEE Trans. Syst. Man, Cybern. Syst.*, vol. 47, no. 7, pp. 1474–1485, Jul. 2017.
- [26] S. Yin, H. Yang, H. Gao, J. Qiu, and O. Kaynak, "An adaptive NN-based approach for fault-tolerant control of nonlinear time-varying delay systems with unmodeled dynamics," *IEEE Trans. Neural Netw. Learn. Syst.*, vol. 28, no. 8, pp. 1902–1913, Aug. 2017.
- [27] M. Hashemi, J. Ghaisari, and J. Askari, "Adaptive control for a class of MIMO nonlinear time delay systems against time varying actuator failures," *ISA Trans.*, vol. 57, pp. 23–42, Jul. 2015.
- [28] Y.-X. Li and G.-H. Yang, "Robust adaptive fault-tolerant control for a class of uncertain nonlinear time delay systems," *IEEE Trans. Syst. Man, Cybern. Syst.*, vol. 47, no. 7, pp. 1554–1563, Jul. 2017.
- [29] H. Ma, H. Ren, Q. Zhou, R. Lu, and H. Li, "Approximation-based Nussbaum gain adaptive control of nonlinear systems with periodic disturbances," *IEEE Trans. Syst. Man, Cybern. Syst.*, vol. 52, no. 4, pp. 2591–2600, Apr. 2022.
- [30] F. L. Lewis, A. Yesildirek, and K. Liu, "Multilayer neural-net robot controller with guaranteed tracking performance," *IEEE Trans. Neural Netw.*, vol. 7, no. 2, pp. 388–399, Mar. 1996.
- [31] T. Bruckner, *Elementary Real Analysis*, 2008.



DANIAL ROSTAMI received the B.S. degree in electrical engineering and the M.S. degree in control and systems engineering from Isfahan University of Technology, Isfahan, Iran, in 2021 and 2024, respectively. His research interests include adaptive control, fault-tolerant control systems, system identification, and time delay systems.



MARZIEH KAMALI received the B.S. degree in biomedical engineering from Amirkabir University of Technology, Tehran, Iran, in 2004, and the M.S. and Ph.D. degrees in control engineering from Isfahan University of Technology, Isfahan, Iran, in 2007 and 2012, respectively. She is currently an Associate Professor with the Department of Electrical and Computer Engineering, Isfahan University of Technology. Her research interests include adaptive control, time delay systems,

multi-agent systems, and fault-tolerant control systems.

...